LIMNOLOGY AND OCEANOGRAPHY
Letters

ASLO
Open Access

Limnology and Oceanography Letters 2020

doi: 10.1002/lol2.10174

LETTER

Continental margin sediments underlying the NE Pacific oxygen minimum zone are a source of nitrous oxide to the water column

Brett D. Jameson[1]* *Peter Berg*[2] *Damian S. Grundle*[3] *Catherine J. Stevens*[1] *S. Kim Juniper*[1,4,5]

[1]School of Earth and Ocean Sciences, Bob Wright Centre, University of Victoria, Victoria, British Columbia, Canada; [2]Department of Environmental Sciences, University of Virginia, Charlottesville, Virginia; [3]Bermuda Institute of Ocean Sciences, St. George's, Bermuda; [4]Department of Biology, University of Victoria, Victoria, British Columbia, Canada; [5]Ocean Networks Canada, Victoria, British Columbia, Canada

Scientific Significance Statement

Nitrous oxide (N_2O) is a potent greenhouse gas that also contributes to stratospheric ozone depletion. Continental margin sediments represent an understudied, yet potentially important marine contributor to global oceanic N_2O budgets. Here, we present an improved method of constraining N_2O production and vertical fluxes in deep-water sediments using trace-level microsensors and mathematical modelling. We demonstrate that continental margin sediments underlying the NE Pacific oxygen minimum zone are a significant source of N_2O to the overlying water column, and that low-oxygen events such as upwelling can stimulate N_2O production in outer shelf sediments. Our data represent the first estimates of sedimentary N_2O production in the NE Pacific and suggest that N_2O efflux is modulated by bottom water oxygen concentrations.

Abstract

Continental margin sediments are important sites of marine nitrogen cycling and potential contributors to atmospheric N_2O emissions. We employed trace-level N_2O microsensors to measure vertical N_2O profiles at submillimeter resolutions in intact cores from outer continental margin sediments underlying the NE Pacific oxygen minimum zone. We used mathematical modeling to estimate depth-dependent rates of N_2O production and fluxes to the overlying water along a transect of diminishing bottom water oxygen concentrations. Net sediment efflux was observed at all sites on the outer continental margin, with a mean value of 524 nmol m^{-2} d^{-1}. N_2O efflux increased with decreased oxygen penetration depth in sediments. Enhanced N_2O production and efflux were obtained when outer continental shelf sediments were experimentally exposed to lower bottom-water O_2 concentrations, to simulate upwelling conditions. Our results underline the need for further

*Correspondence: bjameson@uvic.ca

Associate editor: Henrietta Dulai

Author Contribution Statement: All authors contributed to the conception of the experimental design and data interpretation. BDJ and SKJ collected the sediment cores and performed the incubation experiments aboard the CCSV John P. Tully. BDJ measured pore-water concentration profiles and performed the model analyses. PB provided the PROFILE script and assisted with model interpretations. The manuscript was written by BDJ and edited with the assistance/comments of all authors.

Data Availability Statement: Data are available in the Scholars Portal Dataverse Repository at https://dataverse.scholarsportal.info/dataset.xhtml?persistentId=doi:10.5683/SP2/P58E1E.

Additional Supporting Information may be found in the online version of this article.

investigation of the drivers of N_2O production in continental margin sediments, and the relative importance of these environments to the global N_2O budget.

Nitrous oxide (N_2O) is an important and increasingly abundant atmospheric trace gas which, in the troposphere, has a per mol atmospheric warming potential that is up to 340 times that of CO_2 over a 100-year timespan (Bange, 2008; IPCC 2014). N_2O also survives transport to the stratosphere where it contributes to ozone depletion (IPCC 2014). In terrestrial and aquatic environments, N_2O is produced by nitrifying bacteria and archaea, and both produced and consumed by denitrifying bacteria. Recent estimates indicate that the global ocean acts as a net source of N_2O to the atmosphere, amounting to approximately 25% of the combined 15.8 TgN-N_2O yr^{-1} of natural and anthropogenic emissions (Ciais et al. 2013). Elevated N_2O production rates and atmospheric fluxes are often associated with productive oceanographic regions, such as eastern boundary upwelling systems and mesoscale eddies, where high rates of organic matter decomposition drive steep redox gradients and rapid nitrogen cycling in subsurface waters and sediments (Arévalo-Martínez et al. 2015; Grundle et al. 2017). However, modeled estimates of global oceanic flux have high degrees of uncertainty, partially attributable to sparse observational data coverage across marine environments (Bange et al. 2019). Indeed, studies have primarily focused on water column oxygen minimum zones (OMZs) and estuarine systems (Freing et al. 2012; Murray et al. 2015), leaving data gaps over large portions of the global ocean.

Comparatively little effort has been directed at investigating N_2O cycling in offshore sediments and in relation to the availability of dissolved O_2 in bottom waters. Continental margin sediments are important regions of organic carbon deposition, fueled by high primary production in overlying shelf waters (Huettel et al. 2014). The remineralization of organic matter in surface sediments results in shallow oxygen penetration depths (Devol 2015), and facilitates tight spatial coupling of nitrification and denitrification at the sedimentary oxycline (Devol and Christensen 1993; Seitzinger and Giblin 1996; Devol 2015). This highlights the potential contributions of sedimentary processes to N_2O cycling on the continental margin.

The Northeast Subarctic Pacific Ocean (NESAP) is characterized by an intermediate depth OMZ ($\sim$ 400–1100 m) that impinges on continental slope sediments off the coasts of British Columbia, Washington and Oregon (Crawford and Peña 2013), and N_2O concentrations in the OMZ core can exceed 50 nmol L^{-1} (Fenwick and Tortell 2018). In situ production of N_2O has been attributed to water column nitrification, based on N_2O excess (ΔN_2O) vs. apparent oxygen utilization (AOU) relationships, and the fact that water column dissolved O_2 concentrations in the OMZ core ($\sim$ 10 μmol L^{-1}) remain above the hypothesized threshold for the onset of denitrification (Grundle et al. 2012; Capelle and Tortell 2016; Fenwick and Tortell 2018). However, the status of sediments underlying the NESAP OMZ as sources or sinks of N_2O to the water column has not been investigated. Previous research in the region has confirmed both nitrification and denitrification activity in shelf and slope sediments, with denitrification fueled by nitrate supplied from the overlying water column and from sedimentary nitrification (Devol and Christensen 1993; Belley et al. 2016).

N_2O originating in subsurface waters in this area can be emitted to the atmosphere following episodic upwelling and other vertical mixing processes (Capelle and Tortell 2016), presenting a potential conduit linking N_2O cycling in sediments with sea surface N_2O emissions. In addition, the exposure of shelf sediments to low-O_2 waters during upwelling events or through longer-term shoaling of the upper OMZ may have undescribed impacts on sediment N_2O production and efflux. Dissolved O_2 concentrations below 45 μmol L^{-1} have been observed in bottom waters on the Vancouver Island continental shelf between 200 and 100 m depth during the summer upwelling season, and long-term declines in O_2 concentrations on the continental shelf have been observed in previous decades (Crawford and Peña 2013).

We report the first measurements of submillimeter-scale N_2O pore-water profiles, depth-distributed production rates, and vertical fluxes in offshore sediments using trace-level N_2O microsensors and mathematical modeling. We employed the numerical profile interpretation procedure, PROFILE (Berg et al. 1998), to model N_2O production rates and sediment effluxes in relation to O_2 consumption and bottom water O_2 availability. Our results demonstrate substantial sedimentary N_2O production in the NESAP, and highlight the potential contribution of continental margin sediments to water column N_2O accumulation and sea-to-air emissions.

Methods

Field sampling

Field operations were conducted off the west coast of Vancouver Island, Canada, between 29 September and 04 October 2019. All data are available through Scholars Portal Dataverse (Jameson et al. 2020). A multicorer was used to collect replicate sediment cores (i.d. = 9.8 cm; length = 52.0 cm) from three sampling stations (200, 475, and 850 m depth) positioned along a transect of increasing depth and diminishing bottom water O_2 concentrations (Fig. 1). The two deeper stations (475 and 850 m) were within the portion of the upper

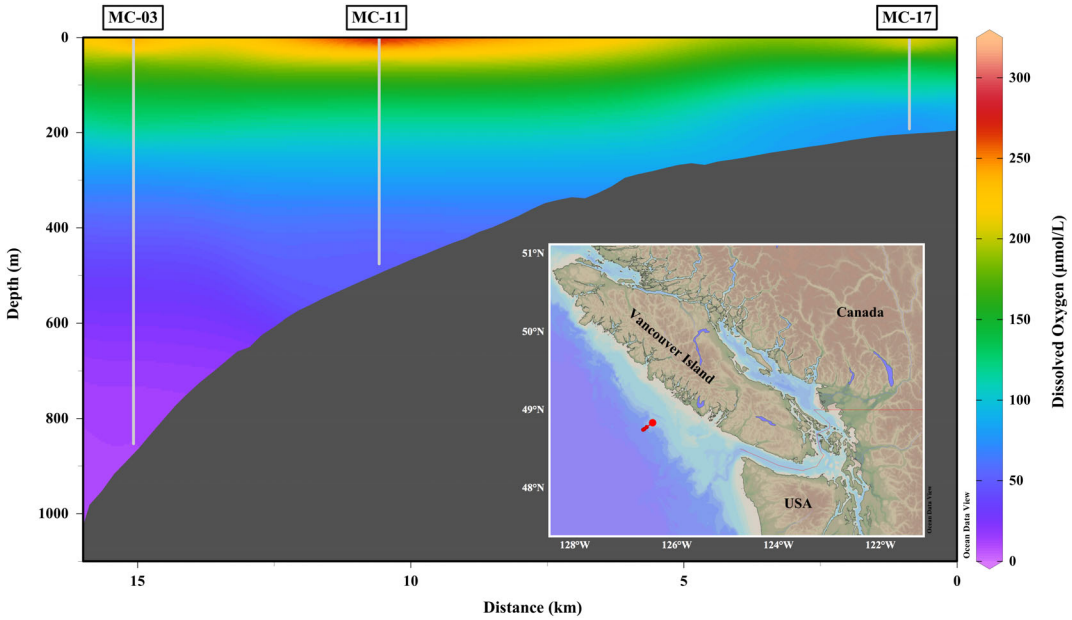

Fig 1. Map of locations selected for multi-core sediment sampling and depth-section of water column dissolved O_2 concentrations. Samples were collected on Clayoquot Slope in the Northeast Pacific between 29 September and 02 October 2019. White lines on the depth-section plot indicate the locations of water column profile and multi-core operations. This figure was created in Ocean Data View using the Data-Interpolating Variational Analysis (DIVA) tool. The interpolation was performed using CTD cast data from four stations, including the three sediment sampling locations labeled above and one off-shelf deep CTD cast station not shown (no sediments were collected at this station).

continental slope that is influenced by the OMZ, whereas the shallowest station (200 m) represented the more oxygenated outer continental shelf. Bottom water characteristics were measured at each station using a CTD rosette (SBE 43, Sea-Bird Electronics), and bottom water samples were obtained from 5 to 10 m above the seafloor in 2.8-L Niskin bottles. We immediately transferred the bottom water to an N_2-flushed reservoir using ¾ inch Tygon tubing and stored it in the shipboard cold room.

Incubation procedures and upwelling experiment

We incubated triplicate sediment cores from each sampling location for 24–36 h under near in situ temperature and dissolved O_2 conditions to reestablish steady-state conditions prior to sediment profiling. Sediment cores were sealed with ~ 1.5 L of bottom-water headspace using acrylic caps fitted with water circulation ports and magnetic stir bars to facilitate continuous water flow and headspace mixing (Belley et al. 2016). Core tubes were connected in line to a peristaltic pump and an oxygen-control reservoir (13.25 L high-density polyethylene; neoprene lid gasket) using 5/8 inch Masterflex Precision Pump Tubing (Cole-Parmer, Montreal, CAN). Water circulation ports, an O_2 measurement port, and a gas control port were fitted into the reservoir lid (Fig. S1). The same setup was used to incubate three additional cores from the 200 m station in low-O_2 water obtained from 475 m depth, to examine how N_2O flux in outer continental shelf sediments might respond to exposure to low-O_2 water during upwelling events. The experiment simulated dissolved O_2 concentrations observed by Ocean Networks Canada (ONC) in continental shelf bottom waters in the region during the summer upwelling season (Crawford and Peña 2013). During the upwelling season, low-O_2 bottom waters can propagate across the shelf to the outer coast of Vancouver Island and are regularly detected at the ONC Folger Deep node at 98 m depth (ONC 2020).

The peristaltic pump continuously circulated water from the reservoir through the core tubes at a flow rate of ~ 50 mL min^{-1}. We maintained steady-state dissolved O_2 concentrations in the headspace water by bubbling either N_2 gas or medical-grade compressed air (Praxair, Mississauga, Ontario) into the reservoir through the gas control port using an aquarium air stone. We monitored O_2 concentrations at regular intervals (2–4 h) in the reservoir using a Fibox 4 Trace O_2 meter; and in individual core tubes with pre-fitted O_2 Sensor Spots using a Fibox Polymer Optical Fiber attachment (PreSens, Regensburg, DE). Temperature in the reservoir was recorded continuously using an RBRduet T.D. Dual Channel Logger (RBR Ltd., Ottawa, Ontario).

In situ bottom water dissolved O_2 ranged from 10 to 77 μmol L^{-1}, temperatures ranged from 4.0°C to 6.9°C, while salinity ranged from 34.0 to 34.3 (PSS-78) (Table 1). All sediment cores were incubated at a mean temperature of 8.2 (± 0.6)°C, over the final 8 h of incubation. Mean O_2 concentrations during the same timeframe were 132.5 (± 15.4), 32.3

Table 1. Sampling stations, dates, locations, and environmental characteristics.

Station	Date	Lat (N)	Long (W)	Depth (m)	Temp (°C)	Salinity (PSS-78)	Bottom O_2 (μmol L^{-1})	Porosity (%)	OPD (mm)
MC-17	28 Sep 2019	48° 49.86	126° 28.99	200	6.9	34.0	77	56±11	4.2 ± 1.1^{C} 1.3 ± 0.2^{U}
MC-11	01 Oct 2019	48° 46.66	126° 35.30	475	5.4	34.1	47	53±3	1.8±0.2
MC-03	02 Oct 2019	48° 45.26	126° 38.31	850	4.0	34.3	10	81±2	0.9±0.1

Temperature, Salinity, and O_2 values are for bottom water at the depth of sediment core collection. OPD = mean oxygen penetration depth in initial profiles (± SE, $n = 3$), defined as the depth at which pore-water O_2 reaches suboxic levels ($O_2 < 5$ μmol L^{-1}). For the 200 m site, superscripts *C* and *U* represent OPDs measured in the control and upwelling cores, respectively. Porosity values are reported as mean values (± SD) for the top 10 mm of sediment.

(± 0.9), 32.8 (± 6.8), and 13.9 (± 4.3) μmol L^{-1}, respectively, for the 200 m control, 200 m upwelling experiment, 475 and 850 m sediment core incubations (Supporting Information Table S2).

Microelectrode profiles

We measured pore-water N_2O and O_2 concentration profiles in post-incubation cores, and in initial cores immediately following sampling (Fig. S2). The latter was to ensure that post-incubation profiles were not artifacts of the incubation procedure. Profiles were obtained using Clark-type N_2O and O_2 microelectrodes with respective detection limits less than 20 nmol L^{-1} and 0.3 μmol L^{-1}, and sensor tip diameters of 500 and 200 μm (Unisense, Aarhus, Denmark). All sensors were calibrated in a CAL300 chamber by two-point calibration according to manufacturer instructions. The O_2 sensor was calibrated in a zero-oxygen solution and in air-saturated water, correcting O_2 concentration of air-saturated water for temperature and salinity (Garcia and Gordon 1992, 1993). The N_2O sensor was calibrated in bottom water flushed with N_2 and 15.6 ppmv N_2O gas standards, and N_2O concentrations in enriched standards were calculated using the N_2O solubility coefficients table (Weiss and Price 1980).

Microelectrodes were mounted on a Unisense MM33 motorized micromanipulator and adjusted to the sediment interface prior to profiling. Discrete measurements were made at 500 μm steps, starting at 1000 μm above the sediment interface and terminating once consistent zero values were reached. N_2O and O_2 profiles were measured separately and sensors were left to equilibrate at each measurement depth in accordance with individual sensor response times (25 and 5 s, respectively).

PROFILE interpretations and statistical analyses

We used pore-water profiles from postincubation cores to model depth-dependent production/consumption rates and sediment fluxes using the numerical profile interpretation procedure PROFILE described by Berg et al. (1998). We determined sediment porosities in each incubated core according to Dalsgaard et al. (2000), for use in the PROFILE model. Oxygen penetration depths (OPD), defined as the depth at which pore-water O_2 fell to less than the suboxic level of 5 μmol L^{-1} (Belley et al. 2016), were estimated in each core following linear interpolation between individual data points. Concentration profile measurements, sediment fluxes and OPDs are all reported as means (± SE, $n = 3$).

We conducted all analyses in the R statistical environment (R Core Team 2019), and tested all datasets for normality using Shapiro–Wilks tests. Where assumptions of linearity or normality were violated, we natural-log transformed the response variable. To determine the potential drivers of N_2O flux variability, we fit a multiple regression to N_2O fluxes using the paired O_2 fluxes and OPDs as predictor variables. Finally, we fit a separate linear regression relating individual OPDs and bottom water (headspace) O_2 concentrations.

Results

Pore-water concentration profiles

Mean OPDs were deepest in the control cores from 200 m depth, where natural bottom water O_2 concentrations were highest, and shallowest in the 850 m cores from the OMZ core (Table 1; Fig. 2). Natural log-transformed OPDs were positively correlated with bottom water (headspace) O_2 concentrations ($R^2_{adj} = 0.46$, $p < 0.01$). We observed pronounced subsurface N_2O maxima coinciding with down-core transitions to suboxic conditions in cores from the 200 m upwelling experiment, 475, and 850 m; while the 200 m control sediments showed relatively consistent concentrations in the top 3 mm (Fig. 2). Maximum pore-water N_2O concentrations ranged from 57 (± 10) in the 200 m control sediments to 116 (± 20) nmol L^{-1} in the 475 m sediments. In the cores from 200 m depth, pore-water N_2O concentrations were higher in experimental (simulated upwelling) cores (78 ± 16 nmol L^{-1}) than in the controls (57 ± 10 nmol L^{-1}).

PROFILE interpretations

Modeled concentration profiles for both N_2O and O_2 provided good fits ($R^2 > 0.98$) to the mean profiles (Fig. 2). Maximum net N_2O production rates coincided with zones of O_2 consumption in surface sediments for all core incubations, and increased with diminishing bottom water O_2

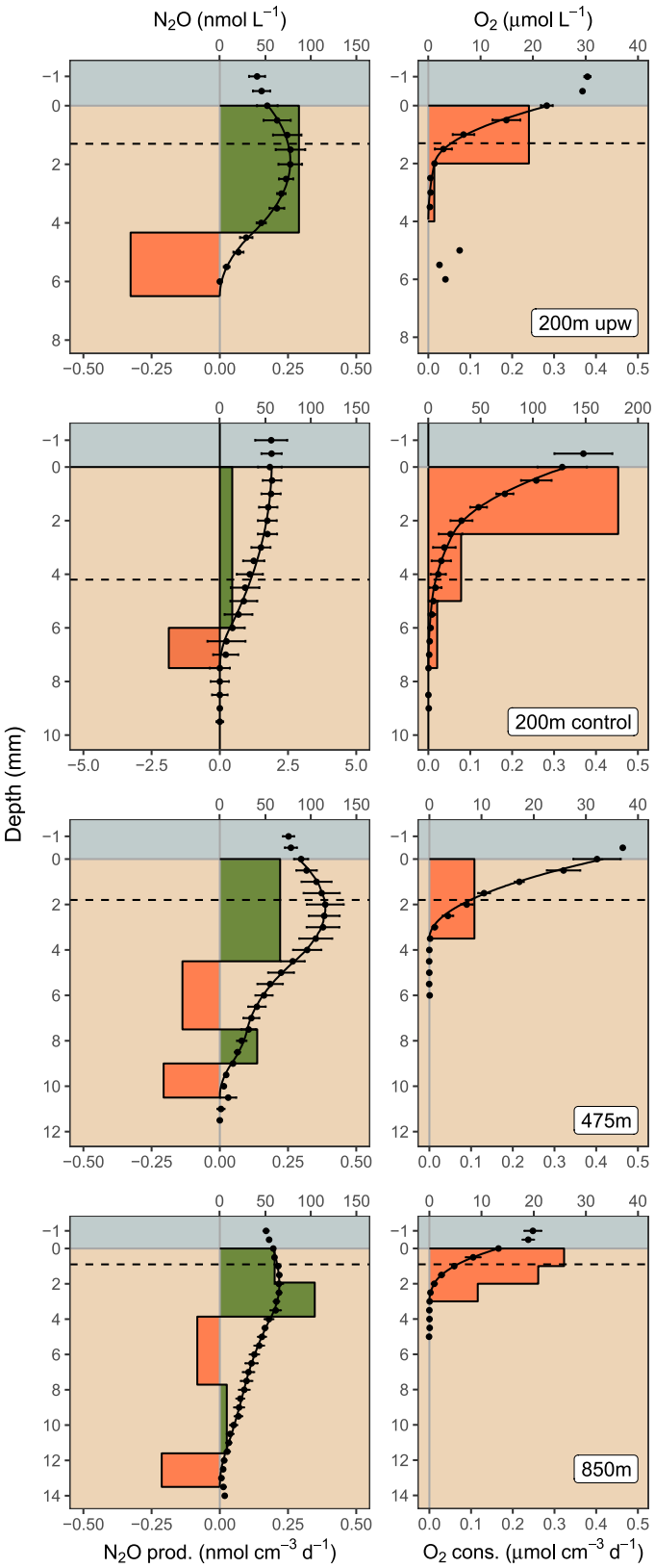

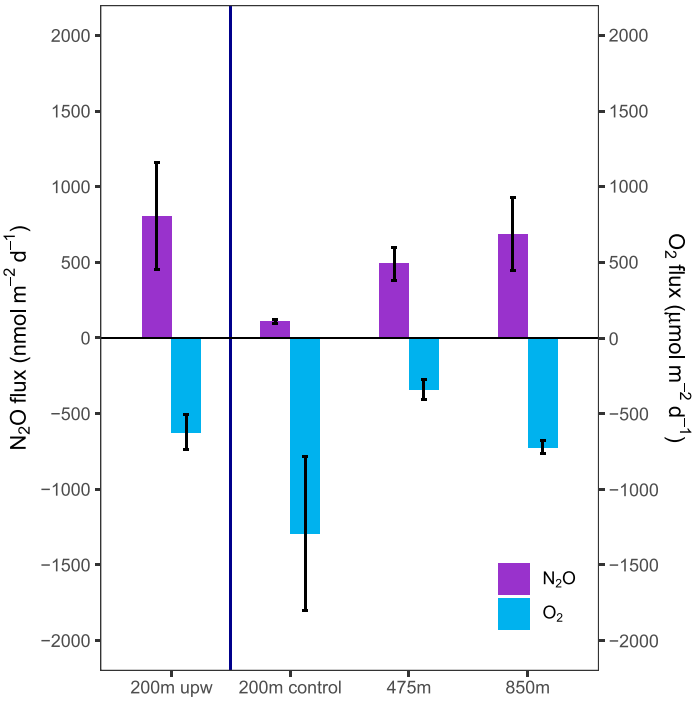

Fig 3. Modeled estimates of N_2O and O_2 sediment fluxes. Values represent mean fluxes (± SE) estimated from individual concentration profiles for the 200 m control (n = 2), 200 m upwelling, 475 m, and 850 m cores (n = 3). Note the 1000 factor difference in units between N_2O fluxes (nmol m^{-2} d^{-1}) and O_2 fluxes (μmol m^{-2} d^{-1}).

concentrations. Maximum N_2O production rates in the 200 m sediments increased from 0.046 to 0.290 nmol cm^{-3} d^{-1} between the control and upwelling cores, while increasing from 0.221 to 0.348 nmol cm^{-3} d^{-1} between the 475 and 850 m cores. Single zones of net consumption coincided with declines in pore-water N_2O concentrations in anoxic layers for both 200 m incubations. In the 475 and 850 m sediments, secondary zones of net N_2O production of smaller magnitude were present in deeper anoxic layers (Fig. 2).

Fig 2. Depth-distribution of N_2O production and O_2 consumption zones modeled from mean pore-water concentration profiles in post-incubation cores. Solid black lines are modeled concentration profiles and individual points represent measured pore-water concentrations (± SE) for the 200 m control (n = 2), 200 m control, 475 m, and 850 m cores (n = 3). Dashed lines represent the mean OPD. Green and red boxes represent zones of production and consumption, respectively. In each panel, the scale on the upper horizontal axes corresponds to pore-water concentrations, while the lower axis corresponds to rates of production and consumption. Note 1000 factor difference in units between N_2O panels (nmol cm^{-3} d^{-1} and nmol L^{-1}) and O_2 panels (μmol cm^{-3} d^{-1} and μmol L^{-1}), and the change in scale for the O_2 concentration axis in the 200 m control profiles.

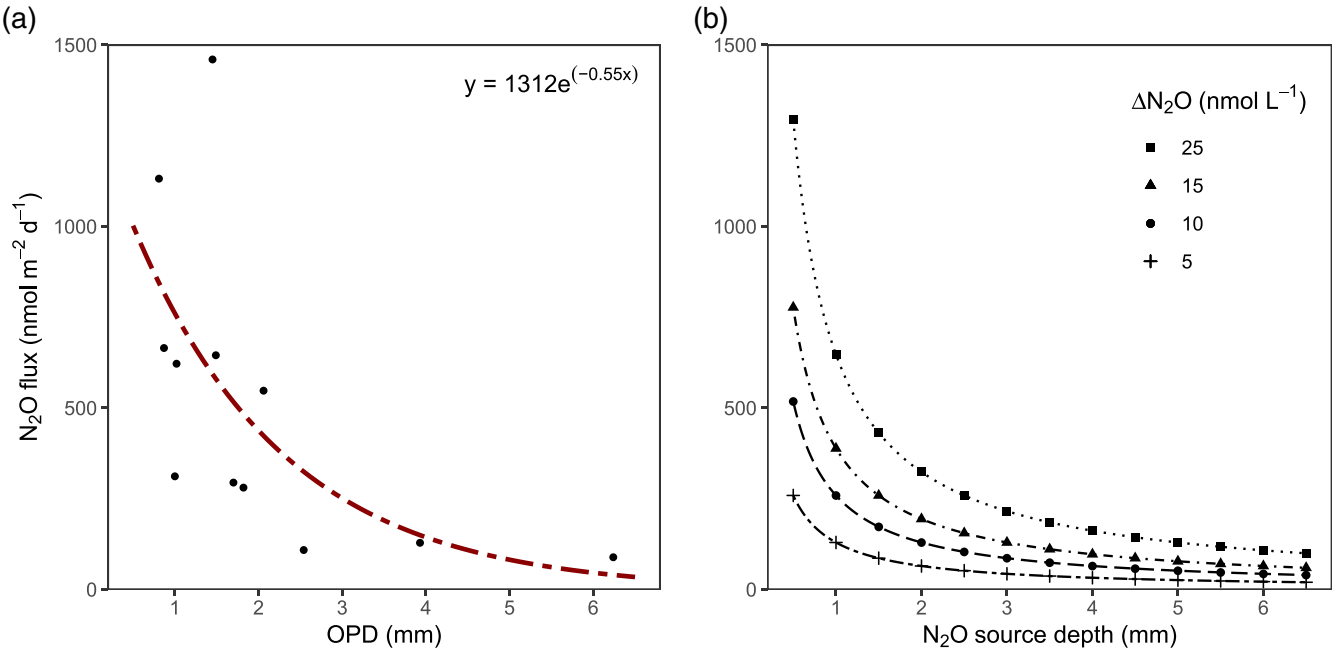

Fig 4. (**a**) N_2O efflux as a function of oxygen penetration depth (OPD). Efflux (nmol m^{-2} d^{-1}) and OPD (mm) values were determined from measured pore-water concentrations in individual cores, pooled across all incubations. The correlation is statistically significant (R^2_{adj} = 0.31, p = 0.035). (**b**) Modeled analysis of the sensitivity of N_2O efflux to N_2O source depth and change in N_2O concentration between the sediment surface and the subsurface N_2O source (ΔN_2O). For each ΔN_2O value, N_2O effluxes (nmol m^{-2} d^{-1}) were calculated from varying N_2O source depths (mm) using Fick's First Law of Diffusion, and holding the sediment diffusivity and porosity constant.

Sediment fluxes

Sediment N_2O effluxes were positive for all sampling locations (Fig. 3). Mean N_2O effluxes were lowest in the 200 m control cores (109 ± 28 nmol m^{-2} d^{-1}) and increased fivefold to a maximum of 806 (± 613) nmol m^{-2} d^{-1} in the 200 m upwelling cores. Mean N_2O effluxes for the 475 and 850 m cores were comparable at 456 (± 248) and 687 (± 413) nmol m^{-2} d^{-1}, respectively. OPD and O_2 flux accounted for approximately 66% of the variability in natural log-transformed N_2O fluxes (R^2_{adj} = 0.66, $p < 0.01$). In separate, nonlinear exponential models, N_2O efflux was inversely correlated with OPD (R^2_{adj} = 0.31, p = 0.035) but was not significantly correlated with O_2 flux (Fig. 4a). Total O_2 consumption estimates ranged from 341 (± 110) to 965 (± 640) μmol m^2 d^{-1} and did not show any discernable trends.

Discussion

This study provides a first examination of N_2O cycling in continental margin sediments of the NESAP, and implicate these environments as net N_2O sources to the overlying water column. Downcore, subsurface N_2O maxima and zones of highest production rates generally corresponded to zones of O_2 consumption, implicating ammonium oxidation as an important production pathway. N_2O production from ammonium oxidation under low-O_2 conditions is the result of incomplete oxidation of the metabolic intermediate, hydroxylamine (Kozlowski et al. 2016), and exponential increases in N_2O production have been demonstrated below 30 μmol L^{-1} O_2 in OMZ waters of the eastern tropical North Pacific (Trimmer et al. 2016). Potential contributions from denitrification are also indicated by the extension of N_2O production zones below the OPD. Denitrification can also proceed under suboxic conditions, and partial denitrification leading to N_2O accumulation has been attributed to the higher O_2 sensitivity of the N_2O-reductase enzyme (Spiro 2012). Further work will be needed to evaluate the relative contributions of nitrification and denitrification to N_2O production in offshore sediments, and how this balance may be related to environmental factors.

The negative correlation of N_2O efflux and OPD observed here (Fig. 4a) suggests that N_2O efflux may be influenced by diffusion distance between zones of production and the sediment surface. To test this, we modeled the sensitivity of N_2O efflux to N_2O source depth by applying Fick's First Law of Diffusion to a hypothetical dataset constrained by our results. Holding sediment diffusivity and porosity constant, we calculated the effect of N_2O concentration gradient strength $\left(\frac{dC}{dX}\right)$ on diffusive fluxes by varying the N_2O source depth and N_2O source concentrations (Fig. 4b). Since subsurface N_2O maxima observed in this study coincided with suboxic sediment depths, we set the range of N_2O source depths to encompass the range of mean OPDs across all incubations. Source concentrations were within the range of those observed in our

cores. These results demonstrate the degree to which N_2O efflux can be influenced by source depth and the resulting strength of concentration gradients, and suggest that there may be a critical OPD beyond which little N_2O can reach the sediment surface unless there are large increases in N_2O production (Fig. 4b).

The results of our simulated upwelling experiment suggest that low-O_2 events can increase N_2O efflux from shelf sediments, through shoaling of the OPD and a rapid metabolic response of N_2O-producing organisms. Bottom-water hypoxia can extend over large portions of the continental shelf during the upwelling season, as low-O_2 water from the offshore OMZ propagates inshore (Grantham et al. 2004). Since upwelling events in the NE Pacific are also associated with large increases in sea surface N_2O emissions (Capelle and Tortell 2016), this creates a possible link between sediment N_2O production and the atmosphere. This also emphasizes the need for additional research into the effects of long-term OMZ shoaling (Crawford and Peña 2013) on sedimentary N_2O production.

Our estimates of N_2O efflux are generally an order of magnitude lower than those reported for intertidal estuarine sediments (Murray et al. 2015). The higher N_2O production rates and sediment efflux in estuaries can be attributed to increased organic matter supply, DIN concentrations, and temperatures (Middelburg et al. 1995; Murray et al. 2015). However, there is considerable spatial and temporal variability in the magnitude and direction of reported N_2O fluxes in estuarine sediments (Murray et al. 2015). This variability has been linked, in part, to DIN availability, with net N_2O consumption by denitrification commonly observed when NO_3^- and NO_2^- are sufficiently low (Jensen et al. 1984; Foster and Fulweiler 2016). The global median NO_3^- concentration for estuarine systems is approximately 50 μmol L^{-1} (Murray et al. 2015), and much of the work on sedimentary N_2O production has focused on eutrophic estuaries, where NO_3^- concentrations can exceed 500 μmol L^{-1} (Sanders et al. 1997). In contrast, bottom water NO_3^- plus NO_2^- concentrations for our sampling sites in September 2019 ranged from 30.19 to 44.84 μmol L^{-1} (Table S1, DFO 2020). As well, Capelle and Tortell (2016) report NO_3^- plus NO_2^- values for the NE Pacific water column that are all below 50 μmol L^{-1}.

Other measurements of N_2O flux in subtidal and offshore sediments have used whole-core squeezing (Usui et al. 1998) or sealed-core incubations (Townsend-Small et al. 2014), both of which limit their use for constraining N_2O effluxes. Pore-water concentration profiles obtained from whole-core squeezing have poor depth resolution and large depth assignment uncertainties (Bender et al. 1987), which can mask small-scale gradients near the sediment interface and bias subsequent flux estimates. Continuous declines in dissolved O_2 during sealed-core incubations could potentially lead to changes in OPD, and cause shifts toward net N_2O consumption as oxygen-limitation becomes more severe (Barnes and Upstill-Goddard 2018). Further, our N_2O efflux estimates are likely conservative, as we were not able to account for bioturbation-enhanced sediment diffusivity (Aller and Aller 1992; Berg et al. 2001). Holding pore-water concentrations constant, any increase in diffusivity would increase modeled rate estimates and associated N_2O effluxes (Berg et al. 1998)

Using data from all stations, we calculate a daily flux of 524 ± 122 nmol N_2O m^{-2} d^{-1} (n = 12) from the sediment to the overlying water column. By comparison, average sea-to-air N_2O flux for the world ocean is approximately 1030 nmol N_2O m^{-2} d^{-1} (Grundle et al. 2012; Ciais et al. 2013), while similar estimates for the Vancouver Island continental margin range from negative efflux prior to summertime upwelling, to a positive efflux of ~7600 nmol N_2O m^{-2} d^{-1} (Grundle et al. 2012; Capelle and Tortell 2016; Fenwick and Tortell 2018). These comparisons underlie the potential importance of continental margin sediments as sources for oceanic N_2O flux to the atmosphere, as well as the need to better constrain regional sources, especially in areas where permanent or temporary low-O_2 conditions enhance conditions for N_2O production in water columns and sediments.

Conclusions

We present the first measurements and estimates of submillimeter-scale pore-water N_2O concentration profiles, depth-distributed production rates, and vertical fluxes in offshore sediments that combine trace-level N_2O microsensor measurements and mathematical modeling. This method provides an improved approach to constraining sediment N_2O cycling in deep-water sediments under steady-state conditions, and requires minimal sediment disturbance. The PROFILE model also allows for an assessment of the vertical positioning of N_2O production zones in relation to sediment oxyclines and the seawater interface. This study has highlighted the importance of continental margin sediments as sources of N_2O to the regional water column in the NE Pacific Ocean, and shown the importance of bottom water O_2 concentrations in modulating N_2O production and effluxes. The results of the simulated upwelling experiment also suggest a dynamic response of N_2O-producing microbes to transient changes in dissolved O_2. Upwelling events may thus contribute additionally to atmospheric N_2O emissions by stimulating sediment N_2O efflux into the water column, a proportion of which may ventilate to the atmosphere as the water masses continue to shoal. These underline the need for further research into the spatial and temporal variability of N_2O production in continental margin sediments, and their relative importance to the global N_2O budget.

Conflict of interest

The authors declared no potential conflicts of interests.

References

Aller, R. C., and J. Y. Aller. 1992. Meiofauna and solute transport in marine muds. Limnol. Oceanogr. **37**: 1018–1033. doi:https://doi.org/10.4319/lo.1992.37.5.1018.

Arévalo-Martínez, D. L., A. Kock, C. R. Löscher, R. A. Schmitz, and H. W. Bange. 2015. Massive nitrous oxide emissions from the tropical South Pacific Ocean. Nat. Geosci. **8**: 530–533. doi:https://doi.org/10.1038/ngeo2469.

Bange, H. W. 2008. Gaseous nitrogen compounds in the ocean, p. 52–84. *In* D. G. Capone, D. A. Bronk, M. R. Mulholland, and E. J. Carpenter [eds.], *Nitrogen in the marine environment*. Elsevier. https://doi.org/10.1016/B978-0-12-372522-6.00002-5.

Bange, H. W., and others. 2019. A harmonized nitrous oxide (N_2O) ocean observation network for the 21st century. Front. Mar. Sci. **6**(157):1–10. doi:https://doi.org/10.3389/fmars.2019.00157.

Barnes, J., and R. C. Upstill-Goddard. 2018. The denitrification paradox: The role of O_2 in sediment N_2O production. Estuar. Coast. Shelf Sci. **200**: 270–276. doi:https://doi.org/10.1016/j.ecss.2017.11.018.

Belley, R., P. V. R. Snelgrove, P. Archambault, and S. K. Juniper. 2016. Environmental drivers of benthic flux variation and ecosystem functioning in Salish Sea and Northeast Pacific sediments. PLoS One **11**: e0151110. doi:https://doi.org/10.1371/journal.pone.0151110.

Bender, M., W. Martin, J. Hess, F. Sayles, L. Ball, and C. Lambert. 1987. A whole-core squeezer for interfacial porewater sampling1. Limnol. Oceanogr. **32**: 1214–1225. doi:https://doi.org/10.4319/lo.1987.32.6.1214.

Berg, P., S. Rysgaard, P. Funch, and M. Sejr. 2001. Effects of bioturbation on solutes and solids in marine sediments. Aquat. Microb. Ecol. **26**: 81–94. doi:https://doi.org/10.3354/ame026081.

Berg, P., N. Risgaard-Petersen, and S. Rysgaard. 1998. Interpretation of measured concentration profiles in sediment pore water. Limnol. Oceanogr. **43**: 1500–1510. doi:https://doi.org/10.4319/lo.1998.43.7.1500.

Capelle, D. W., and P. D. Tortell. 2016. Factors controlling methane and nitrous-oxide variability in the southern British Columbia coastal upwelling system. Mar. Chem. **179**: 56–67. doi:https://doi.org/10.1016/j.marchem.2016.01.011.

Ciais, P., and others. 2013. Carbon and other biogeochemical cycles. *In* T. F. Stocker, and others [eds.], *Climate change 2013: The physical science basis. Contribution of Working Group I to the Fifth Assessment Report of the Intergovernmental Panel on Climate Change*. Cambridge, UK: Cambridge Univ. Press.

Crawford, W. R., and M. A. Peña. 2013. Declining oxygen on the British Columbia continental shelf. Atmos.-Ocean **51**: 88–103. doi:https://doi.org/10.1080/07055900.2012.753028.

Dalsgaard, T. 2000. Protocol handbook for NICE - Nitrogen Cycling in Estuaries: a project under the EU research programme: Marine Science and Technology (MAST III). p. 62. *In* L. P. Nielsen, and others [eds.], National Environmental Research Institute: Silkeborg, Denmark.

Devol, A. H. 2015. Denitrification, anammox, and N_2 production in marine sediments. Ann. Rev. Mar. Sci. **7**: 403–423. doi:https://doi.org/10.1146/annurev-marine-010213-135040.

Devol, A. H., and J. P. Christensen. 1993. Benthic fluxes and nitrogen cycling in sediments of the continental margin of the eastern North Pacific. J. Mar. Res. **51**: 345–372. doi:https://doi.org/10.1357/0022240933223765.

DFO. 2020. Institute of Ocean Sciences Data Archive. Ocean Sciences Division. Department of Fisheries and Oceans Canada, [accessed 2020 September 15]. Available from http://www.pac.dfo-mpo.gc.ca/science/oceans/data-donnees/index-eng.html

Fenwick, L., and P. D. Tortell. 2018. Methane and nitrous oxide distributions in coastal and open ocean waters of the Northeast Subarctic Pacific during 2015–2016. Mar. Chem. **200**: 45–56. doi:https://doi.org/10.1016/j.marchem.2018.01.008.

Foster, S. Q., and R. W. Fulweiler. 2016. Sediment nitrous oxide fluxes are dominated by uptake in a temperate estuary. Front. Mar. Sci. **3**(40): 1–13. https://doi.org/10.3389/fmars.2016.00040.

Freing, A., D. W. R. Wallace, and H. W. Bange. 2012. Global oceanic production of nitrous oxide. Philos. Trans. R. Soc. B: Biol. Sci. **367**: 1245–1255. doi:https://doi.org/10.1098/rstb.2011.0360.

Garcia, H. E., and L. I. Gordon. 1993. Erratum: Oxygen solubility in seawater: Better fitting equations. Limnol. Oceanogr. **38**: 656.

Garcia, H. E., and L. I. Gordon. 1992. Oxygen solubility in seawater: Better fitting equations. Limnol. Oceanogr. **37**: 1307–1312. doi:https://doi.org/10.4319/lo.1992.37.6.1307.

Grantham, B. A., F. Chan, K. J. Nielsen, D. S. Fox, J. A. Barth, A. Huyer, J. Lubchenco, and B. A. Menge. 2004. Upwelling-driven nearshore hypoxia signals ecosystem and oceanographic changes in the northeast Pacific. Nature **429**: 749–754. doi:https://doi.org/10.1038/nature02605.

Grundle, D. S., C. R. Löscher, G. Krahmann, M. A. Altabet, H. W. Bange, J. Karstensen, A. Körtzinger, and B. Fiedler. 2017. Low oxygen eddies in the eastern tropical North Atlantic: Implications for N_2O cycling. Sci. Rep. **7**: 4806. doi:https://doi.org/10.1038/s41598-017-04745-y.

Grundle, D. S., R. Maranger, and S. K. Juniper. 2012. Upper water column nitrous oxide distributions in the northeast subarctic Pacific Ocean. Atmos.-Ocean **50**: 475–486. doi:https://doi.org/10.1080/07055900.2012.727779.

Huettel, M., P. Berg, and J. E. Kostka. 2014. Benthic exchange and biogeochemical cycling in permeable sediments. Ann. Rev. Mar. Sci. **6**: 23–51. doi:https://doi.org/10.1146/annurev-marine-051413-012706.

IPCC. 2014. Climate Change 2014: Synthesis Report. Contribution of Working Groups I, II and III to the Fifth Assessment Report of the Intergovernmental Panel on Climate Change [Core Writing Team, R.K. Pachauri and L.A. Meyer (eds.)]. IPCC, Geneva, Switzerland, 151 pp.

Jameson, B. D., P. Berg, D. S. Grundle, C. J. Stevens, and S. K. Juniper. 2020. Data from: Continental margin sediments underlying the NE Pacific oxygen minimum zone are a source of nitrous oxide to the water column. https://doi.org/10.5683/SP2/P58E1E, Scholars Portal Dataverse, V1, UNF:6:AzQ3jlzHwjPg/9q9FQNp/w== [fileUNF].

Jensen, H. B., K. S. Jørgensen, and J. Sørensen. 1984. Diurnal variation of nitrogen cycling in coastal, marine sediments. Mar. Biol. **83**: 177–183. doi:https://doi.org/10.1007/BF00394726.

Kozlowski, J. A., K. D. Kits, and L. Y. Stein. 2016. Comparison of nitrogen oxide metabolism among diverse ammonia-oxidizing bacteria. Front. Microbiol. **7**(1090): 1–9. https://doi.org/10.3389/fmicb.2016.01090.

Middelburg, J. J., G. Klaver, J. Nieuwenhuize, R. M. Markusse, T. Vlug, and F. J. W. A. van der Nat. 1995. Nitrous oxide emissions from estuarine intertidal sediments. Hydrobiologia **311**: 43–55. doi:https://doi.org/10.1007/BF00008570.

Murray, R. H., D. V. Erler, and B. D. Eyre. 2015. Nitrous oxide fluxes in estuarine environments: Response to global change. Global Change Biol. **21**: 3219–3245. doi:https://doi.org/10.1111/gcb.12923.

ONC. 2020. Folger Passage - Folger Deep dissolved oxygen data. Oceans Networks Canada, University of Victoria, Canada, [accessed 2020 June 30]. Available from https://www.oceannetworks.ca/observatories/pacific/folger-passage#SOO-FP

R Core Team. 2019. *R: A language and environment for statistical computing*. Vienna, Austria: R Foundation for Statistical Computing, Available from https://www.R-project.org/.

Sanders, R. J., and others. 1997. Nutrient fluxes through the Humber estuary. J. Sea Res. **37**: 3–23. doi:https://doi.org/10.1016/S1385-1101(96)00002-0.

Seitzinger, S. P., and A. E. Giblin. 1996. Estimating denitrification in North Atlantic continental shelf sediments, p. 235–260. *In* R. W. Howarth [ed.], *Nitrogen cycling in the North Atlantic Ocean and its watersheds*. Netherlands: Springer. doi:https://doi.org/10.1007/978-94-009-1776-7_7.

Spiro, S. 2012. Nitrous oxide production and consumption: Regulation of gene expression by gas-sensitive transcription factors. Philos. Trans. R. Soc. B: Biol. Sci. **367**: 1213–1225. doi:https://doi.org/10.1098/rstb.2011.0309.

Townsend-Small, A., M. G. Prokopenko, and W. M. Berelson. 2014. Nitrous oxide cycling in the water column and sediments of the oxygen minimum zone, eastern subtropical North Pacific, Southern California, and Northern Mexico (23°N–34°N). J. Geophys. Res.: Oceans **119**: 3158–3170. doi:https://doi.org/10.1002/2013JC009580.

Trimmer, M., Chronopoulou, P.-M., Maanoja, S. T., Upstill-Goddard, R. C., Kitidis, V., & Purdy, K. J. 2016. Nitrous oxide as a function of oxygen and archaeal gene abundance in the North Pacific. Nat. Commun., **7**, 13451. https://doi.org/10.1038/ncomms13451

Usui, T., I. Koike, and N. Ogura. 1998. Vertical profiles of nitrous oxide and dissolved oxygen in marine sediments. Mar. Chem. **59**: 253–270. doi:https://doi.org/10.1016/S0304-4203(97)00091-1.

Weiss, R. F., and B. A. Price. 1980. Nitrous oxide solubility in water and seawater. Mar. Chem. **8**: 347–359. doi:https://doi.org/10.1016/0304-4203(80)90024-9.

Acknowledgments

This research was supported by the Canadian Healthy Oceans Network (CHONe), Ocean Networks Canada (ONC), the University of Victoria, and the Bermuda Institute of Ocean Sciences. We would like to thank the Snelgrove Lab and Memorial University of Newfoundland, especially Vanessa Reid and Alessia Ciraolo, who provided the equipment for sediment core incubations and assisted with sample collection and core incubations. We would also like to thank Dr. Steve Mihaly for his assistance with deck operations, as well as the Captain and crew of the CCGS John P. Tully. Finally, we would like to thank Drs. Roberta Hamme and Réal Roy for their valued input on the first manuscript drafts.

Submitted 06 July 2020
Revised 23 September 2020
Accepted 22 October 2020